

CT-Guided Core Needle Biopsy of Nonspinal Bone Lesions: Comparison of Occult and Visible Bone Lesions

Wonsuk Kim, MD^{1,2}, Kevin Sun, MD¹, Justin W. Kung, MD¹, Jim S. Wu, MD¹

Musculoskeletal Imaging · Original Research

Keywords

bone, core needle biopsy, CT guided, diagnostic yield, occult

Submitted: Apr 13, 2022

Revision requested: Apr 25, 2022

Revision received: May 24, 2022

Accepted: Jun 15, 2022

First published online: Jun 22, 2022

Version of record: Oct 12, 2022

Based on a presentation at the Society of Skeletal Radiology 2022 annual meeting, Coronado, CA.

An electronic supplement is available online at doi.org/10.2214/AJR.22.27842.

The authors declare that there are no disclosures relevant to the subject matter of this article.

BACKGROUND. CT guidance may be used for biopsy of indeterminate bone lesions detected by MRI or PET/CT that are not visible (i.e., occult) on CT owing to equipment-, patient-, and operator-related factors.

OBJECTIVE. The purpose of this study was to assess diagnostic yield (DY) and diagnostic performance of CT-guided core needle biopsy (CNB) of occult nonspinal bone lesions and to identify the most common benign and malignant diagnoses for occult lesions undergoing CNB.

METHODS. This retrospective study included 1033 adult patients who underwent CT-guided nonspinal bone CNB between January 2004 and December 2020. Lesions were classified as occult or visible on CT; biopsies of occult lesions were performed by targeting anatomic landmarks using prebiopsy MRI or PET/CT. Pathologic results of CNB were classified as diagnostic or nondiagnostic to calculate DY of CNB. For nondiagnostic CNBs, final diagnoses were established by subsequent pathologic, clinical, and imaging follow-up.

RESULTS. The sample included 70 patients with occult lesions (mean age, 56.8 years; 38 women, 32 men) and 963 patients with visible lesions (mean age, 59.6 years; 475 women, 488 men). Malignancy rate was lower for occult than for visible lesions (42.9% vs 60.9%, $p = .004$). DY was lower for occult than for visible lesions (37.1% vs 76.9%, $p < .001$). Diagnostic performance for detecting malignancy on the basis of final diagnoses was lower for occult than for visible lesions in terms of sensitivity (76.7% vs 93.7%, $p = .003$), specificity (7.9% vs 56.5%, $p < .001$), and accuracy (38.2% vs 80.0%, $p < .001$). Final diagnoses among malignant occult and visible lesions included metastasis (frequencies of 63.3% vs 65.4%), leukemia/lymphoma (33.3% vs 11.6%), and myeloma (3.3% vs 10.4%); final diagnoses among benign occult and visible lesions included red marrow (34.2% vs 8.2%), reactive marrow (26.3% vs 11.8%), and fracture (18.4% vs 3.8%). Occult lesions detected by MRI versus PET/CT had lower malignancy rate (39.3% vs 68.0%, $p = .03$) and lower DY (30.4% vs 60.0%, $p = .01$).

CONCLUSION. At CT-guided CNB, malignancy rate and DY are lower for occult than for visible lesions. Leukemia/lymphoma and red marrow are more common among occult than visible lesions.

CLINICAL IMPACT. Understanding these characteristics can help guide radiologists', referring providers', and patients' expectations when CNB of occult bone lesions is requested and performed.

CT-guided core needle biopsy (CNB) is a valuable tool in the diagnosis and management of suspicious or indeterminate nonspinal bone lesions. Though surgical biopsy is considered the reference standard for diagnosis, image-guided CNB is preferred because of its lower complication rate, less invasive nature, lower cost, and shorter recovery times [1–4]. For experienced operators, CNB can decrease the need for surgical intervention and assist surgical planning [5–9]. The reported diagnostic yield (DY), defined as the number of diagnostic biopsies divided by the total number of biopsies, of CNB for visible bone lesions is well documented and ranges from 69% to 93% [2, 4, 10–22]. CNBs are more likely to be nondiagnostic in cases of osteomyelitis, small lesions, spinal lesions, benign and low-grade neoplasms, lymphoma, and sclerotic lesions [1, 5, 10, 11, 13, 22–24].

Suspicious or indeterminate nonspinal bone lesions that are detected by MRI, PET/CT, or bone scintigraphy may appear occult on radiography and CT (hereafter, occult lesions) and,

ARRS is accredited by the Accreditation Council for Continuing Medical Education (ACCME) to provide continuing medical education activities for physicians.

The ARRS designates this journal-based CME activity for a maximum of 1.00 AMA PRA Category 1 Credit™. Physicians should claim only the credit commensurate with the extent of their participation in the activity.

To access the article for credit, follow the prompts associated with the online version of this article.

doi.org/10.2214/AJR.22.27842

AJR 2023; 220:104–114

ISSN-L 0361–803X/23/2201–104

© American Roentgen Ray Society

¹Department of Radiology, Beth Israel Deaconess Medical Center, Boston, MA.

²Present affiliation: Rayus Radiology, 115 NE 100th St, Ste 101, Seattle, WA 98125. Address correspondence to W. Kim (wonsuk.kim@cdird.com).

therefore, may be difficult to target on CT-guided biopsy [25]. Although MRI-compatible biopsy equipment is available, scanner availability, operator experience, and patient factors (e.g., pacemaker, other implantable device, or claustrophobia) can limit its use [26–28]. PET/CT-guided biopsies are also constrained by availability, expertise, and increase in both procedure time and excess radiation exposure for the operator and support staff [29, 30]. Radiologists experienced in CT-guided biopsies may prefer to instead biopsy occult lesions under CT guidance using anatomic landmarks with respect to the prior imaging that showed the lesion. However, the DY of CT-guided biopsies of occult lesions is not well established, being evaluated by only a single study to our knowledge [25]; in that study, biopsy results were concordant with final histopathologic results in 90% of both occult and visible lesions. In addition, the spectrum of diagnoses that are likely to be encountered when biopsying lesions that are occult on CT is not well established. We therefore conducted this study to assess the DY and diagnostic performance of CT-guided CNB of occult nonspinal bone lesions and to identify the most common benign and malignant diagnoses for occult lesions that undergo CNB.

Methods

Patient Selection

This retrospective study was HIPAA compliant and received institutional review board approval. The requirement for written informed consent was waived. The study was conducted at a single tertiary academic center with a specialized orthopedic oncology service. The service maintains a prospective database of nonspinal musculoskeletal biopsies performed in adults. This database was searched to identify consecutive patients who underwent CT-guided nonspinal CNB between January 2004 and December 2020, yielding 1462 patients. Patients were then excluded if the CNB was nontargeted (e.g., a bone marrow aspiration) ($n = 177$) or did not target bone (e.g., biopsy of a soft-tissue lesion without osseous involvement) ($n = 252$). These exclusions resulted in a final study sample of 1033 patients. All biopsies of occult lesions were performed during follow-up after the lesions were detected on an earlier CT, MRI, PET/CT, or bone scintigraphy examination.

HIGHLIGHTS

Key Finding

■ At CT-guided CNB, occult, versus visible, lesions had a lower malignancy rate (42.9% vs 60.9%, $p = .004$) and lower DY (37.1% vs 76.9%, $p < .001$). Diagnoses more common among occult than visible lesions included leukemia/lymphoma (33.3% vs 11.6% of final malignant diagnoses) and red marrow (34.2% vs 8.2% of final benign diagnoses).

Importance

■ Knowledge of expected outcomes of CNB of occult bone lesions can help triage biopsy requests and guide expectations for the radiologist, referring provider, and patient.

CT-Guided Core Needle Biopsy Technique

All CNBs were performed under CT fluoroscopy guidance by one of 18 fellowship-trained musculoskeletal radiologists with 2–17 years of posttraining experience. A fellow in musculoskeletal imaging typically participated in the biopsy procedures. For lesions found to be occult on CT at the time of biopsy, the target location on CT was determined using anatomic landmarks with reference to the lesion’s location on the prebiopsy MRI and/or PET/CT examinations that detected the lesion. A 13- or 15-gauge bone biopsy system (Bonopty, AprioMed) or coaxial (11-gauge access needle, 13-gauge biopsy needle) battery-powered bone access system (OnControl, Vidacare) was used. A minimum of three cores were obtained to optimize DY (mean, 4.2 cores; maximum, eight cores) [31]. Spring-loaded soft-tissue needles may have been used to biopsy lesions with an extraosseous soft-tissue component or very lytic lesions but not to biopsy occult lesions. For patients with clinically suspected osteomyelitis, additional samples were sent for microbiology analysis. All pathology specimens from the CNBs were reviewed by institutional musculoskeletal pathologists.

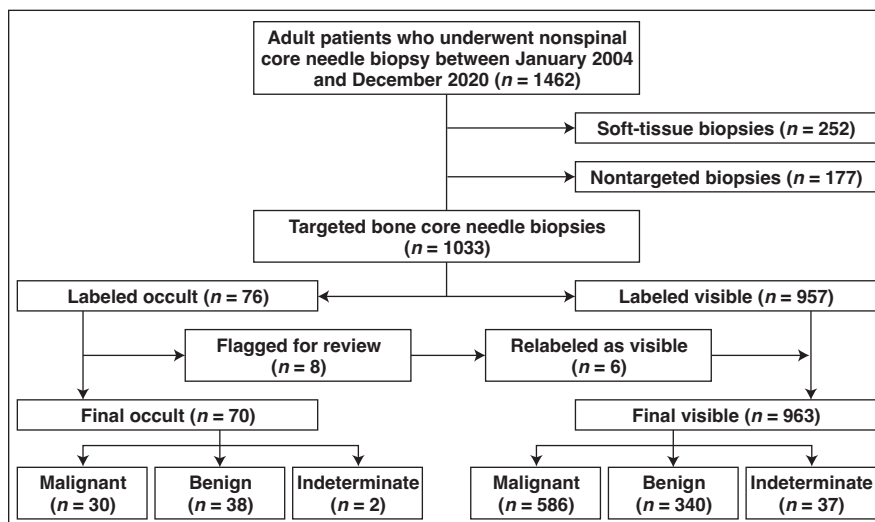


Fig. 1—Flowchart shows selection of patients who underwent CT-guided core needle biopsies.

TABLE 1: Summary of Patient Characteristics

| Characteristic | Occult Lesions (n = 70) | Visible Lesions (n = 963) | p ^a |
|-----------------------------|-------------------------|---------------------------|----------------|
| Age (y), mean ± SD | 56.8 ± 17.3 | 59.6 ± 16.4 | .69 |
| Sex | | | .93 |
| Female | 38 (54.3) | 475 (49.3) | |
| Male | 32 (45.7) | 488 (50.7) | |
| Known history of malignancy | 41 (58.6) | 403 (41.8) | .008 |

Note—Unless otherwise indicated, data represent number of patients with percentage in parentheses.

^aBold value is statistically significant ($p < .05$).

Retrospective Review of Occult Lesions

At the time of biopsy, the radiologist performing the biopsy documented in the database whether the targeted lesion was occult, sclerotic, lytic, or mixed. On the basis of the documented classification, the targeted lesions were classified as occult or visible (encompassing sclerotic, lytic, or mixed). For lesions classified in the database as occult, two musculoskeletal radiologists (J.S.W. and W.K., with 17 and 5 years of posttraining experience, respectively) independently reviewed the CT images obtained during the biopsy procedures to confirm that the lesion was occult and to assess the accuracy of biopsy targeting. During this review, a lesion was considered occult if visible cortical changes, periosteal reaction, or internal matrix different from the adjacent marrow was absent on CT. No explicit criteria were used for assessing accuracy of biopsy targeting. Any differences between the two radiologists were resolved by discussion. If a lesion that was originally documented in the database as occult was instead considered visible at the time of this retrospective review, then the lesion was classified as visible for all remaining analyses.

Data Collection

Patient age at the time of biopsy, patient sex, known history of malignancy, lesion location (classified as central [nonextremity, such as sacrum] vs peripheral [extremity, such as humerus, femur, or more distal bones]), and specific bone biopsied were recorded for all lesions. For occult lesions, the prior imaging modality that detected the lesion (MRI and/or PET/CT) was recorded. One of the previously noted investigators (J.S.W.) reviewed all available clinical notes, pathology reports, and surgical reports to classify each CNB as diagnostic or nondiagnostic. The CNB was considered diagnostic if the sample tissue revealed a distinct pathologic

diagnosis that was consistent with the imaging and clinical diagnosis, corresponding to the definition of diagnostic biopsy in numerous earlier studies [18, 24, 31–34]. If a definitive diagnosis was not attained by pathology from the CNB, then the CNB was considered nondiagnostic. All CNBs with malignant results were considered diagnostic. CNBs with nonmalignant benign neoplastic results (e.g., fibrous dysplasia, giant cell tumor of bone, or enchondroma) were also considered diagnostic. Other nonmalignant results were classified as diagnostic or nondiagnostic on a case-by-case basis depending on the nature of the pathology report (i.e., if the pathology report characterized the diagnosis as definitive) and the correlation of the diagnosis with the imaging and clinical findings.

For nondiagnostic biopsies, the previously noted investigator (J.S.W.) reviewed all available subsequent clinical notes and results of subsequent biopsies and imaging examinations to determine a final diagnosis for the lesion. The follow-up interval was defined as the time between the CNB and the last available subsequent biopsy, clinical note, or imaging examination. A final malignant diagnosis could be recorded on the basis of any subsequent pathologic results regardless of the follow-up interval. After a nondiagnostic biopsy, a final benign diagnosis of red marrow, reactive marrow, stress fracture, or osteomyelitis typically required a follow-up interval of 12 months but could be established earlier with supporting clinical and/or imaging evidence (e.g., decrease in size or resolution of the lesion). Although any available microbiology culture results were reviewed, a positive culture result was not required to establish a final diagnosis of osteomyelitis. The final diagnosis was classified as indeterminate in patients who were lost to follow-up (i.e., an available follow-up interval of < 12 months) before establishment of a final diagnosis.

TABLE 2: Summary of Malignancy Rates and Measures of Diagnostic Performance

| Characteristic | Occult Lesions | Visible Lesions | p ^a |
|-------------------------|----------------|-----------------|------------------|
| Malignancy rate | 42.9 (30/70) | 60.9 (586/963) | .004 |
| Diagnostic yield | 37.1 (26/70) | 76.9 (741/963) | < .001 |
| Detection of malignancy | | | |
| Sensitivity | 76.7 (23/30) | 93.7 (549/586) | .003 |
| Specificity | 7.9 (3/38) | 56.5 (192/340) | < .001 |
| Accuracy | 38.2 (26/68) | 80.0 (741/926) | < .001 |

Note—Data represent percentage with numerator and denominator in parentheses. Patients with indeterminate lesions are included in derivation of malignancy rate and diagnostic yield but not in derivation of sensitivity, specificity, and accuracy.

^aBold values are statistically significant ($p < .05$).

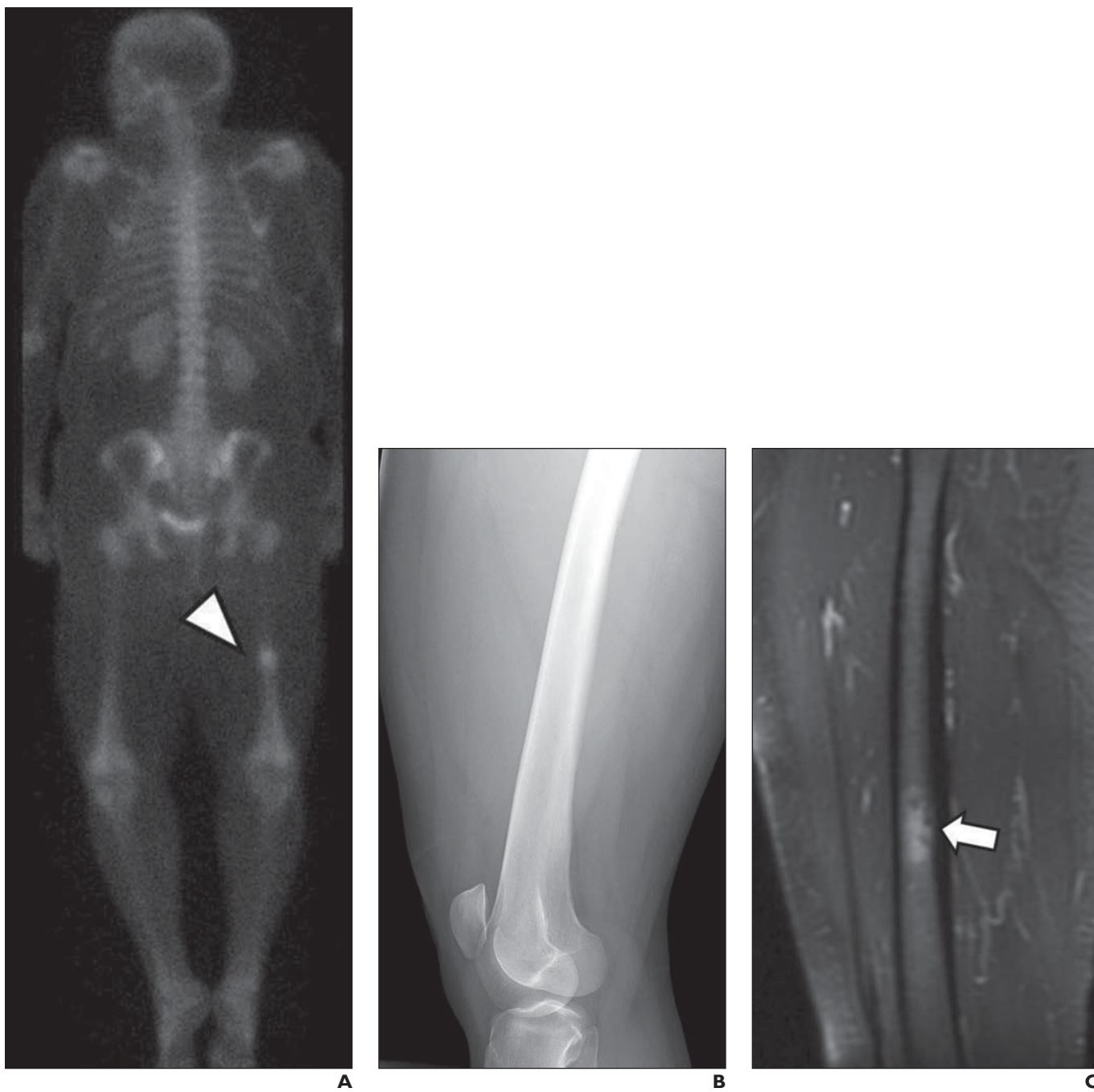


Fig. 2—48-year-old woman with history of breast cancer who presented with left thigh pain.
A, Whole-body bone scintigraphy shows increased radiotracer uptake (*arrowhead*) in left femoral mid diaphysis.
B, Lateral radiograph of distal femur does not show correlative abnormality.
C, Sagittal STIR MR image shows correlative hyperintense lesion (*arrow*) at femoral mid diaphysis. CT-guided core needle biopsy was requested. Lesion was occult on CT at time of biopsy.
D, Axial CT image from core needle biopsy shows biopsy needle in lesion, which was targeted according to anatomic landmarks with respect to prior imaging. Biopsy revealed breast carcinoma metastasis and was considered diagnostic.

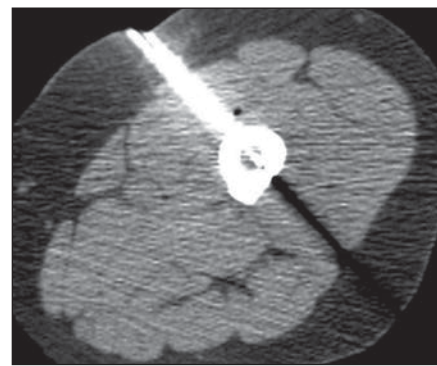


TABLE 3: Summary of Distributions of Lesion Locations and Bones Involved

| Location | Occult Lesions (n = 70) | Visible Lesions (n = 963) | p ^a |
|------------|-------------------------|---------------------------|------------------|
| Central | 25 (35.7) | 554 (57.5) | < .001 |
| Clavicle | 1 (1.4) | 24 (2.5) | |
| Iliac bone | 19 (27.1) | 324 (33.6) | |
| Ischium | 0 (0.0) | 21 (2.2) | |
| Pubic bone | 0 (0.0) | 20 (2.1) | |
| Rib | 2 (2.9) | 49 (5.1) | |
| Sacrum | 1 (1.4) | 46 (4.8) | |
| Scapula | 0 (0.0) | 33 (3.4) | |
| Sternum | 2 (2.9) | 37 (3.8) | |
| Peripheral | 45 (64.3) | 409 (42.5) | < .001 |
| Femur | 27 (38.6) | 177 (18.4) | |
| Fibula | 0 (0.0) | 14 (1.5) | |
| Foot | 0 (0.0) | 14 (1.5) | |
| Hand | 0 (0.0) | 4 (0.4) | |
| Humerus | 14 (20.0) | 84 (8.7) | |
| Patella | 0 (0.0) | 4 (0.4) | |
| Radius | 0 (0.0) | 5 (0.5) | |
| Tibia | 4 (5.7) | 97 (10.1) | |
| Ulna | 0 (0.0) | 10 (1.0) | |

Note—Data are expressed as number of patients with percentage in parentheses.
^aBold values are statistically significant ($p < .05$).

Post Hoc Assessment of Lesions With a Final Diagnosis of Red Marrow

After completion of the initial data analysis, the other previously noted investigator (W.K.) performed a post hoc assessment of all lesions with a final diagnosis of red marrow. The investigator reviewed any available prebiopsy in- and opposed-phase MRI sequence of the lesion to characterize that sequence's impact on the evaluation of the lesion. Findings were summarized descriptively.

Statistical Analysis

Mean patient age was compared between occult and visible lesions using a *t* test. Patients' sex and known history of malignancy were compared between occult and visible lesions using the Fisher exact test. The frequency of a final malignant diagnosis was compared between occult and visible lesions and between patients with and without a known malignancy in both occult and visible lesion groups using the Fisher exact test. The DY was calculated as the ratio of diagnostic CNBs (regardless of whether the final diagnosis was benign or malignant) to the total number of CNBs. The sensitivity, specificity, and accuracy of CNB in detecting malignancy were determined. For this purpose, true-positives were defined as lesions with a malignant final diagnosis and a diagnostic CNB with a malignant result, true-negatives as lesions with a benign final diagnosis and a diagnostic CNB with a benign result, false-positives as lesions with a benign final diagnosis and a nondiagnostic CNB, and false-negatives as lesions with a malignant final diagnosis and a nondiagnostic CNB. The DY, sensitivity, specificity, and accuracy

were compared between occult and visible lesions using the Fisher exact test. The most common malignant and benign final diagnoses for occult and visible lesions were tabulated, stratified according to whether lesions were diagnosed by the initial CNB or during follow-up. The distribution of lesion locations (central vs peripheral) and specific bones biopsied as well as the DY stratified by location and specific bone biopsied were summarized for occult and visible lesions; the distributions and DY were compared between occult and visible lesions stratified by peripheral and central location using the Fisher exact test. For occult lesions, the malignancy rate and DY were compared between lesions visible only on MRI and those visible only on PET/CT using the Fisher exact test. Lesions that were considered indeterminate because patients were lost to follow-up were included in assessments of malignancy rates and DY but excluded from determinations of sensitivity, specificity, and most common benign diagnoses. The significance level for all comparisons was set at $p < .05$. Statistical analysis was performed using Stata (version 13.1, StataCorp).

Results

Retrospective Review of Occult Lesions

Of the 1033 included patients who underwent CNB, 76 had lesions that were documented as occult in the database. At retrospective review of these 76 lesions, eight were deemed visible by at least one of the two radiologists. After discussion, six lesions were reclassified as visible for further analyses, and two lesions remained classified as occult. Thus, after the retrospective review,

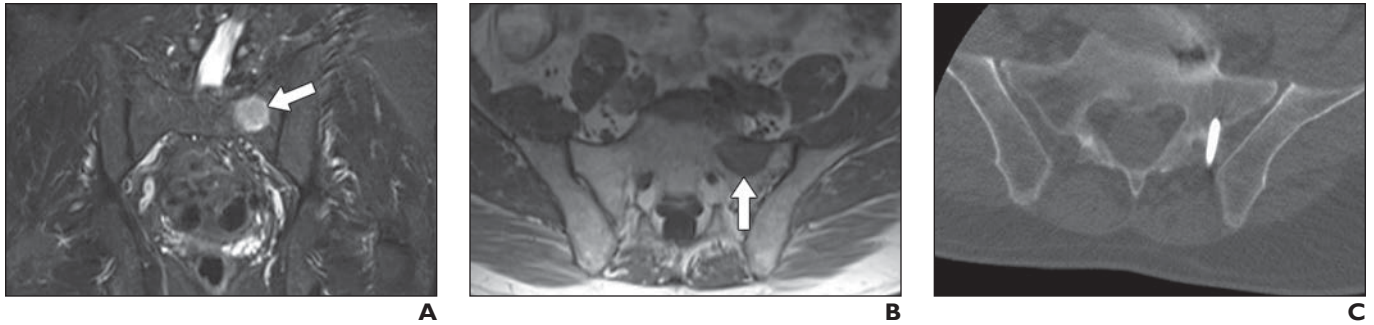


Fig. 3—60-year-old man without history of malignancy who presented with back pain. **A**, Coronal T2-weighted fat-suppressed MR image shows hyperintense left sacral lesion (arrow). **B**, Axial T1-weighted MR image shows hypointensity of lesion (arrow). CT-guided core needle biopsy was requested. Lesion was occult on CT at time of biopsy. **C**, Axial CT image from core needle biopsy shows biopsy needle in lesion, which was targeted according to anatomic landmarks with respect to prior imaging. Biopsy revealed T-cell lymphoma and was considered diagnostic.

6.8% (70/1033) of lesions were considered occult on CT, and the remaining 93.2% (963/1033) of lesions were considered visible on CT. Neither investigator considered any occult lesion to have been missed by the CT-guided CNB.

Patient Characteristics

Figure 1 shows the flow of patient selection, and Table 1 summarizes patient characteristics. Of the 963 patients with visible lesions, the mean age was 59.6 ± 16.4 (SD) years (range, 18–95 years); 49.3% (475/963) were women, and 50.7% (488/963) were men. Of the 70 patients with occult lesions, the mean age was 56.8 ± 17.3 years

(range, 21–88 years); 54.3% (38/70) were women, and 45.7% (32/70) were men. Age and sex were not significantly different between patients with occult and visible lesions (both *p* > .05). A known history of malignancy was more common in patients with occult lesions than in those with visible lesions (58.6% vs 41.8%, *p* = .008).

Summary of Final Diagnoses

CNB was diagnostic in 26 of the 70 occult lesions. Of the 26 occult lesions that were diagnostic on CNB, 23 were malignant, and three were benign. Of the 44 occult lesions that were nondiagnostic on CNB, the mean follow-up interval was 6.7 years (range,

TABLE 4: Diagnostic Yield, Stratified by Lesion Location and Bone Involved

| Location | Occult Lesions | Visible Lesions | <i>p</i> ^a |
|------------|----------------|-----------------|-----------------------|
| Central | 48.0 (12/25) | 80.5 (446/554) | < .001 |
| Clavicle | 0.0 (0/1) | 66.7 (16/24) | |
| Iliac bone | 52.6 (10/19) | 82.1 (266/324) | |
| Ischium | — | 81.0 (17/21) | |
| Pubic bone | — | 85.0 (17/20) | |
| Rib | 0.0 (0/2) | 77.6 (38/49) | |
| Sacrum | 100.0 (1/1) | 78.3 (36/46) | |
| Scapula | — | 84.8 (28/33) | |
| Sternum | 50.0 (1/2) | 75.7 (28/37) | |
| Peripheral | 31.1 (14/45) | 72.1 (295/409) | < .001 |
| Femur | 37.0 (10/27) | 75.7 (134/177) | |
| Fibula | — | 57.1 (8/14) | |
| Foot | — | 57.1 (8/14) | |
| Hand | — | 50.0 (2/4) | |
| Humerus | 21.4 (3/14) | 72.6 (61/84) | |
| Patella | — | 100.0 (4/4) | |
| Radius | — | 80.0 (4/5) | |
| Tibia | 25.0 (1/4) | 71.1 (69/97) | |
| Ulna | — | 50.0 (5/10) | |

Note—Data are expressed as percentage with numerator and denominator in parentheses. Dash (—) indicates diagnostic yield could not be computed because no biopsies targeted the listed bone.

^aBold values are statistically significant (*p* < .05).

0.7–15.5 years); the final diagnosis was malignant in seven, benign in 35, and indeterminate in two. Thus, when considering results from the initial CNB and from the follow-up intervals were considered, the occult lesions comprised 30 malignant lesions, 38 benign lesions, and two indeterminate lesions.

CNB was diagnostic in 741 of the 963 visible lesions. Of the 741 visible lesions that were diagnostic on CNB, 549 were malignant and 192 were benign. For the 222 visible lesions that were non-diagnostic on CNB, the mean follow-up interval was 7.5 years (range, 0.4–16.4 years); the final diagnosis was malignant in 37, benign in 148, and indeterminate in 37. Thus, when results from the initial CNB and from the follow-up interval were considered, the visible lesions comprised 586 malignant lesions, 340 benign lesions, and 37 indeterminate lesions.

The frequency of a final malignant diagnosis (whether attained from the initial CNB or from the subsequent follow-up) was significantly lower for occult than for visible lesions (42.9% vs 60.9%, $p =$

.004). A final malignant diagnosis was significantly more common in patients with than in those without a known history of malignancy for both occult (53.7% [22/41] vs 27.6% [8/29], $p = .049$) and visible (78.9% [318/403] vs 47.5% [266/560], $p < .001$) lesions.

Diagnostic Performance

Table 2 summarizes diagnostic performance. The DY was significantly lower for occult (37.1% [26/70]) than for visible (76.9% [741/963]) lesions ($p < .001$). Diagnostic performance measures for detecting malignancy on the basis of final diagnoses were significantly lower for occult than for visible lesions in terms of sensitivity (76.7% vs 93.7%, $p = .003$), specificity (7.9% vs 56.5%, $p < .001$), and accuracy (38.2% vs 80.0%, $p < .001$).

Most Common Final Diagnoses

The most common final diagnoses are summarized in Tables S1–S4 (available in the [online supplement](#)). All malignant occult

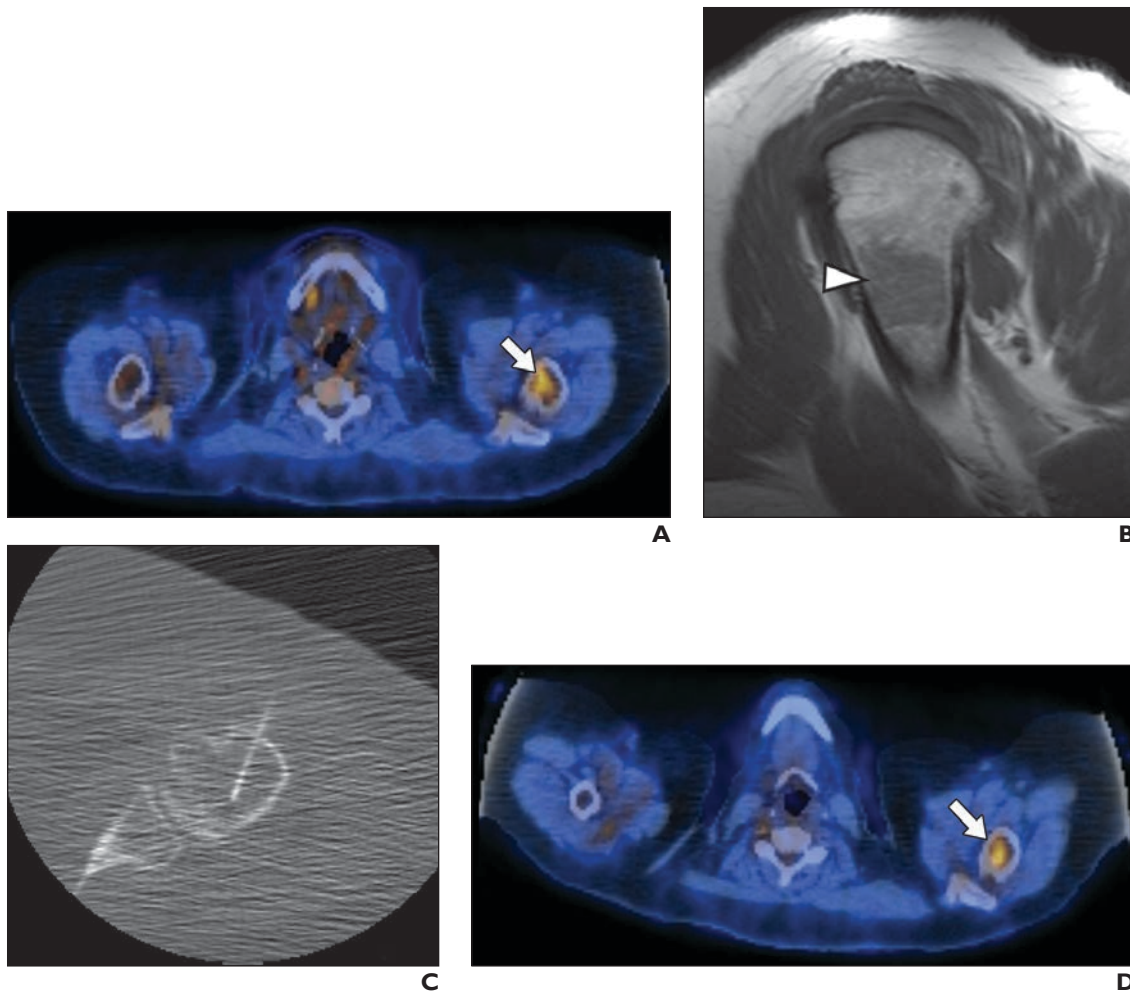


Fig. 4—62-year-old woman with lymphoma and colon cancer who presented for oncology surveillance.

A, Axial image from FDG PET/CT shows increased FDG avidity (*arrow*) in proximal humerus. MRI was performed for further evaluation.

B, Sagittal T1-weighted MR image shows overall hypointensity of lesion (*arrowhead*), though mild hyperintensity relative to skeletal muscle, suggestive of red marrow. CT-guided core needle biopsy was requested, partly owing to patient anxiety and history of two malignancies. Lesion was occult on CT at time of biopsy.

C, Axial CT image from core needle biopsy shows biopsy needle in lesion, which was targeted according to anatomic landmarks with respect to prior imaging. Pathologic report described mildly hypercellular marrow with maturing trilineage hematopoiesis but no malignancy.

D, Axial fused image from FDG PET/CT performed 7 years after biopsy shows persistent uptake in lesion (*arrow*), appearing similar to baseline FDG PET/CT examination in **A**. Five FDG PET/CT examinations performed over course of 8 years after biopsy revealed no change in lesion. Final diagnosis was classified as red marrow given long-term stability.

lesions were diagnosed as metastasis (63.3%), leukemia/lymphoma (33.3%), or myeloma (3.3%). In malignant occult lesions, diagnoses by CNB were metastasis in 65.2%, leukemia/lymphoma in 30.4%, and myeloma in 4.3%. In malignant occult lesions, diagnoses by later follow-up were metastasis in 57.2% and leukemia/lymphoma in 42.9%. Figure 2 shows an occult lesion with a final diagnosis of breast cancer metastasis, and Figure 3 shows an occult lesion with a final diagnosis of T-cell lymphoma.

The most common final diagnoses in malignant visible lesions were metastasis (65.4%), leukemia/lymphoma (11.6%), myeloma (10.4%), and primary sarcoma (10.4%). In malignant visible lesions, diagnoses by CNB were metastasis in 67.9%, leukemia/lymphoma in 10.7%, myeloma in 10.4%, and primary sarcoma in 9.8%. In malignant visible lesions, diagnoses by later follow-up were metastasis in 29.7%, leukemia/lymphoma in 29.7%, primary sarcoma in 27.0%, and myeloma in 5.4%.

The most common final diagnoses in benign occult lesions were red marrow (34.2%), reactive marrow (26.3%), stress fracture (18.4%), and osteomyelitis (13.2%). The three benign occult lesions diagnosed by CNB were osteonecrosis ($n = 2$) and osteomyelitis ($n = 1$). In benign occult lesions, diagnoses by later follow-up were red marrow in 37.2%, reactive marrow in 28.6%, stress fracture in 20.0%, and osteomyelitis in 11.4%. Figure 4 shows an occult lesion with a final diagnosis of red marrow, and Figure 5 shows an occult lesion with a final diagnosis of stress fracture. In one occult lesion, the final diagnosis was osteoid osteoma; the nidus in this lesion did not become visible until follow-up CT performed 4 months after the CNB (Fig. S1, available in the [online supplement](#)).

The most common final diagnoses in benign visible lesions were reactive marrow (11.8%), osteomyelitis (11.5%), fibrous lesion (9.7%), red marrow (8.2%), and giant cell tumor (7.9%). Fracture was diagnosed in 3.8% of visible lesions. In benign visible lesions, diagnoses by CNB were giant cell tumor in 12.5%, osteomyelitis in 12.0%, fibrous lesion in 10.9%, enchondroma in 8.3%, and re-

active marrow in 7.8%. In benign visible lesions, diagnoses by later follow-up were reactive marrow in 16.9%, red marrow in 12.8%, osteomyelitis in 10.8%, and fibrous lesion in 8.1%.

Microbiology cultures were obtained at the time of CNB because of clinically suspected osteomyelitis in 13 occult lesions, one of which was positive for infection, and in 170 visible lesions, 22 of which were positive for infection.

Lesion Locations

Table 3 summarizes the distribution of lesion locations. A peripheral (rather than central) location was significantly more common for occult than visible lesions (64.3% vs 42.5%, $p < .001$). The most common locations for occult lesions were the femur (38.6%), iliac bone (27.1%), and humerus (20.0%), and for visible lesions were the iliac bone (33.6%), femur (18.4%), and tibia (10.1%).

Table 4 presents the DY, stratified by lesion location. The DY was significantly lower for occult than for visible lesions for both central (48.0% vs 80.5%, $p < .001$) and peripheral (31.1% vs 72.1%, $p < .001$) locations. Of sites with at least 10 occult lesions, the DY of occult lesions was 52.6% in the iliac bone, 37.0% in the femur, and 21.4% in the humerus.

Detection of Occult Lesions by Prior Imaging

Of the 70 occult lesions, 56 were detected by MRI, 25 by PET/CT, and 11 by both modalities. The malignancy rate was significantly lower for lesions detected only by MRI than for those detected only by PET/CT (39.3% [22/56] vs 68.0% [17/25], $p = .03$). The DY was significantly lower for lesions detected only by MRI than for those detected only by PET/CT (30.4% [17/56] vs 60.0% [15/25], $p = .01$).

Post Hoc Assessment of Lesions With a Final Diagnosis of Red Marrow

Post hoc assessment was performed for lesions with a final diagnosis of red marrow. A preoperative in- and opposed-phase



Fig. 5—70-year-old man with history of Hodgkin lymphoma who presented with left hip pain.

A, Coronal T1-weighted MR image shows hypointense lesion (arrows) in left acetabulum. CT-guided core needle biopsy was requested. Lesion was occult on CT at time of biopsy.

B, Axial CT image from core needle biopsy shows biopsy needle in lesion, which was targeted according to anatomic landmarks with respect to prior imaging. Biopsy revealed cortical and woven bone with fibrosis but no malignancy.

C, Coronal T1-weighted image from MRI performed 5 years after biopsy shows improvement of acetabular lesion (arrow) and new stress fracture (arrowhead) in left femoral neck. Fixation hardware (star) is present in right femur for osteoporotic femoral neck fracture that occurred 2 years after biopsy. Final diagnosis of left acetabular lesion was classified as stress fracture.

MRI sequence was available for one of the 13 occult lesions with a final diagnosis of red marrow. For that single lesion, the in- and opposed-phase sequence had been considered inconclusive at the time of clinical interpretation, contributing to the decision to perform CNB. A preoperative in- and opposed-phase MRI sequence was available for three of the 28 visible lesions with a final diagnosis of red marrow. However, signal dropout could not be adequately assessed in any of these three lesions because of small lesion size ($n = 2$) and motion artifact ($n = 1$).

Discussion

In this study, we compared CT-guided CNBs performed in occult and visible nonspinal bone lesions. The DY as well as the sensitivity, specificity, and accuracy for malignancy were all significantly lower for CNBs of occult lesions than CNBs of visible lesions. Differences were observed in the spectrums of final diagnoses for the two groups of lesions. For example, occult lesions, in comparison with visible lesions, more commonly had a final malignant diagnosis of leukemia/lymphoma and a final benign diagnosis of red marrow. The malignancy rate and DY were both higher for occult lesions detected only by PET/CT than those detected only by MRI. These findings may provide useful information when considering whether to perform CNB of an occult lesion.

The results of the current study differ from the results of the study by Hillen et al. [25], which showed a DY of 90% for both 30 occult lesions and 30 visible lesions. This discrepancy in results may relate to differences between studies in patient demographics, lesion composition, and definitions of a diagnostic biopsy. For example, in the Hillen et al. study, 87% of patients with occult lesions had a prior diagnosis of malignancy, compared with 58.6% of patients in the current study. In addition, 57% of occult lesions were diagnosed as metastases in their study, compared with 27% in the current study. Establishing a diagnosis by CNB is easier in malignant lesions, in particular for metastases, than in benign lesions [2, 18, 22]; thus, the high rate of metastases among occult lesions in the study by Hillen et al. would be expected to contribute to a higher DY. The occult lesions in the current study also included a relatively high percentage of leukemia/lymphoma cases, which can be difficult to diagnose by CNB, thus lowering DY [2, 10]. Another contributor to the low DY in the current study is the stringent definition of a diagnostic biopsy. CNBs were considered nondiagnostic unless a distinct pathologic diagnosis was provided in the pathology report that was consistent with the imaging and clinical diagnosis. Examples of pathologic results that were treated as diagnostic in the study by Hillen et al. include no abnormality, necrosis, normal hematopoietic cells, and no malignancy; however, in the current study, these would have been classified as nondiagnostic on CNB and thus would have required adequate follow-up for a final diagnosis [25].

In the current study, the malignancy rate was higher in visible than in occult lesions. By definition, occult lesions show no visible cortical injury or medullary change. Such processes are likely to represent indolent nonaggressive disorders. Nonetheless, an aggressive process will be occult early in its pathogenesis, before manifestation of visible bone injury. Metastasis was the most common malignant diagnosis for both occult and visible lesions. Nonetheless, leukemia/lymphoma was a more common diagnosis for occult than visible lesions, consistent with leukemia/lym-

phoma being a medullary process with potentially limited or no cortical involvement.

Red marrow was more common among occult than visible benign lesions and represented the most common benign diagnosis for occult lesions. Red marrow is not expected to cause cortical changes and is commonly visualized by MRI and PET/CT. We cannot entirely exclude the possibility that lesions with a final diagnosis of red marrow or a comparable benign entity (e.g., reactive marrow, stress fracture, or osteomyelitis) instead represented sampling error in the context of a missed malignancy. However, in the case of red marrow, when the initial CNB was nondiagnostic, a final diagnosis was only established after documenting at least 12 months of stability on follow-up imaging (in the absence of a decrease in size or resolution).

A known history of malignancy was more common for occult than for visible lesions. This difference may relate to all occult lesions having been detected by MRI and/or PET/CT before the CNB, with PET/CT being a widely performed test in the evaluation of patients with known malignancy. The known malignancy history would have increased the clinical suspicion for an osseous metastasis and likely influenced the decision to perform CNB despite the lack of a visible lesion. Moreover, occult lesions had a significantly higher frequency of a final malignant diagnosis when detected by PET/CT than by MRI, corresponding to the widespread use of PET/CT in oncologic patients.

Occult lesions accounted for only 6.8% of all CT-guided CNBs. However, given growing indications for the use of MRI and PET/CT in oncologic patients, requests for biopsy of occult lesions will likely increase [35–39]. Knowledge of the DY for CNB of occult lesions, as well as the most common benign and malignant final diagnoses after CNB of occult lesions, can help triage biopsy requests and guide expectations for the radiologist, referring provider, and patient. For instance, biopsies of occult lesions more commonly were associated with a final diagnosis of red marrow than were biopsies of visible lesions. If not already available, an in- and opposed-phase MRI sequence of the occult lesion could be acquired to assess for intralésional fat and potentially avoid an unnecessary biopsy. Insight into common benign diagnoses of occult lesions (e.g., red marrow, stress fracture, and osteomyelitis) may also help guide management decisions if the patient has symptoms consistent with such diagnoses. Finally, occult lesions are more likely to be malignant in patients with a known history of malignancy; thus, a repeat biopsy or close follow-up should be considered when CNB of an occult lesion is nondiagnostic in such patients.

Limitations of this study warrant mention. First, this study was retrospective. A prospective study would be challenging to perform given the infrequency of occult lesions and the requirement for long-term follow-up to establish final diagnoses for lesions that are nondiagnostic on CNB. Second, the study was performed at one institution. Institutional patient populations and referral patterns are expected to impact the results. For instance, the DY would likely be higher in institutions performing CNB primarily in patients with known malignancy. Third, we did not evaluate CNB of bone lesions in children or of spinal lesions, as the musculoskeletal radiology division at our institution does not routinely perform such procedures. It is unclear how inclusion of such biopsies would affect the observed malignancy rate and DY. One

study showed relatively low DY for spinal biopsies, though a different study showed relatively high DY [11, 20]. Finally, the 1033 biopsies were performed by 18 different radiologists over a 17-year study period, and variability in biopsy technique could affect DY. However, all operators were fellowship trained, and at least three core samples were obtained from each lesion.

In conclusion, CT-guided CNB of nonspinal bone lesions that are occult on CT, in comparison with CT-guided CNB of those that are visible on CT, is associated with a significantly lower malignancy rate; significantly lower DY; and significantly lower sensitivity, specificity, and accuracy for malignancy. Diagnoses that were more common in occult than in visible lesions included leukemia/lymphoma and red marrow. Nonetheless, metastasis was the most common malignant diagnosis for both occult and visible lesions. Occult lesions were more likely malignant when detected by only PET/CT than by only MRI. Understanding these characteristics can help guide expectations by radiologists, referring providers, and patients when requesting and performing CT-guided CNB of occult bone lesions.

Provenance and review: Not solicited; externally peer reviewed.

References

- Tsukushi S, Nishida Y, Yamada Y, Yoshida M, Ishiguro N. CT-guided needle biopsy for musculoskeletal lesions. *Arch Orthop Trauma Surg* 2010; 130:699–703
- Dupuy DE, Rosenberg AE, Punyaratabandhu T, Tan MH, Mankin HJ. Accuracy of CT-guided needle biopsy of musculoskeletal neoplasms. *AJR* 1998; 171:759–762
- Tomasian A, Hillen TJ, Jennings JW. Bone biopsies: what radiologists need to know. *AJR* 2020; 215:523–533
- Pohlig F, Kirchhoff C, Lenze U, et al. Percutaneous core needle biopsy versus open biopsy in diagnostics of bone and soft tissue sarcoma: a retrospective study. *Eur J Med Res* 2012; 17:29
- Traina F, Errani C, Toscano A, et al. Current concepts in the biopsy of musculoskeletal tumors. *J Bone Joint Surg Am* 2015; 97:e7
- Kattapuram SV, Rosenthal DI. Percutaneous biopsy of skeletal lesions. *AJR* 1991; 157:935–942
- Gogna A, Peh WC, Munk PL. Image-guided musculoskeletal biopsy. *Radiol Clin North Am* 2008; 46:455–473
- Bickels J, Jelinek JS, Shmookler BM, Neff RS, Malawer MM. Biopsy of musculoskeletal tumors: current concepts. *Clin Orthop Relat Res* 1999; 368:212–219
- Espinosa LA, Jamadar DA, Jacobson JA, et al. CT-guided biopsy of bone: a radiologist's perspective. *AJR* 2008; 190:[web]W283–W289
- Chang CY, Huang AJ, Bredella MA, et al. Percutaneous CT-guided needle biopsies of musculoskeletal tumors: a 5-year analysis of non-diagnostic biopsies. *Skeletal Radiol* 2015; 44:1795–1803
- Hau A, Kim I, Kattapuram S, et al. Accuracy of CT-guided biopsies in 359 patients with musculoskeletal lesions. *Skeletal Radiol* 2002; 31:349–353
- McKay RR, Zukotynski KA, Werner L, et al. Imaging, procedural and clinical variables associated with tumor yield on bone biopsy in metastatic castration-resistant prostate cancer. *Prostate Cancer Prostatic Dis* 2014; 17:325–331
- Cronin CG, Cashell T, Mhuirchearthaigh JN, et al. Bone biopsy of new suspicious bone lesions in patients with primary carcinoma: prevalence and probability of an alternative diagnosis. *AJR* 2009; 193:[web]W407–W410
- Rimondi E, Rossi G, Bartalena T, et al. Percutaneous CT-guided biopsy of the musculoskeletal system: results of 2027 cases. *Eur J Radiol* 2011; 77:34–42
- Li Y, Du Y, Luo TY, et al. Factors influencing diagnostic yield of CT-guided percutaneous core needle biopsy for bone lesions. *Clin Radiol* 2014; 69:e43–e47
- Datir A, Pechon P, Saifuddin A. Imaging-guided percutaneous biopsy of pathologic fractures: a retrospective analysis of 129 cases. *AJR* 2009; 193:504–508
- Hwang S, Lefkowitz RA, Landa J, et al. Percutaneous CT-guided bone biopsy: diagnosis of malignancy in lesions with initially indeterminate biopsy results and CT features associated with diagnostic or indeterminate results. *AJR* 2011; 197:1417–1425
- Didolkar MM, Anderson ME, Hochman MG, et al. Image guided core needle biopsy of musculoskeletal lesions: are nondiagnostic results clinically useful? *Clin Orthop Relat Res* 2013; 471:3601–3609
- Issakov J, Flusser G, Kollender Y, Merimsky O, Lifschitz-Mercer B, Meller I. Computed tomography-guided core needle biopsy for bone and soft tissue tumors. *Isr Med Assoc J* 2003; 5:28–30
- Lis E, Bilsky MH, Pisinski L, et al. Percutaneous CT-guided biopsy of osseous lesion of the spine in patients with known or suspected malignancy. *AJNR* 2004; 25:1583–1588
- Yang J, Frassica FJ, Fayad L, Clark DP, Weber KL. Analysis of nondiagnostic results after image-guided needle biopsies of musculoskeletal lesions. *Clin Orthop Relat Res* 2010; 468:3103–3111
- Omura MC, Motamedi K, UyBico S, Nelson SD, Seeger LL. Revisiting CT-guided percutaneous core needle biopsy of musculoskeletal lesions: contributors to biopsy success. *AJR* 2011; 197:457–461
- Leffler SG, Chew FS. CT-guided percutaneous biopsy of sclerotic bone lesions: diagnostic yield and accuracy. *AJR* 1999; 172:1389–1392
- Ní Mhuirchearthaigh J, McMahon C, Lin YC, Wu J. Diagnostic yield of percutaneous biopsy for sclerotic bone lesions: influence of mean Hounsfield units. *Clin Imaging* 2017; 46:53–56
- Hillen TJ, Talbert RJ, Friedman MV, et al. Biopsy of CT-occult bone lesions using anatomic landmarks for CT guidance. *AJR* 2017; 209:214–221
- Sequeiros RB, Fritz J, Ojala R, Carrino JA. Percutaneous magnetic resonance imaging-guided bone tumor management and magnetic resonance imaging-guided bone therapy. *Top Magn Reson Imaging* 2011; 22:171–177
- Alanen J, Keski-Nisula L, Blanco-Sequeiros R, Tervonen O. Cost comparison analysis of low-field (0.23 T) MRI- and CT-guided bone biopsies. *Eur Radiol* 2004; 14:123–128
- Wu HTH, Chang CY, Chang H, et al. Magnetic resonance imaging guided biopsy of musculoskeletal lesions. *J Chin Med Assoc* 2012; 75:160–166
- Klaeser B, Wiskirchen J, Wartenberg J, et al. PET/CT-guided biopsies of metabolically active bone lesions: applications and clinical impact. *Eur J Nucl Med Mol Imaging* 2010; 37:2027–2036
- Govindarajan MJ, Nagaraj KR, Kallur KG, Sridhar PS. PET/CT guidance for percutaneous fine needle aspiration cytology/biopsy. *Indian J Radiol Imaging* 2009; 19:208–209
- Wu JS, Goldsmith JD, Horwich PJ, Shetty SK, Hochman MG. Bone and soft-tissue lesions: what factors affect diagnostic yield of image-guided core-needle biopsy? *Radiology* 2008; 248:962–970
- Cohen MG, McMahon CJ, Kung JW, Wu JS. Comparison of battery-powered and manual bone biopsy systems in core needle biopsy of sclerotic bone lesions. *AJR* 2016; 206:[web]W83–W86
- Wu JS, McMahon CJ, Lozano-Calderon S, Kung JW. Utility of core needle rebiopsy of initially non-diagnostic musculoskeletal lesions. *AJR* 2017; 208:609–616
- Thavikulwat AC, Wu JS, Chen X, Anderson ME, Ward A, Kung J. Image-guided core needle biopsy of adipocytic tumors: diagnostic accuracy and concordance with final surgical pathology. *AJR* 2021; 216:997–1002
- Ul-Hassan F, Cook GJ. PET/CT in oncology. *Clin Med (Lond)* 2012; 12:368–372
- Li J, Zhou H, Zhang X, Song F, Pang X, Wei Z. A two-way comparison of whole-body ¹⁸F PET-CT and whole-body contrast-enhanced MRI for dis-

- tant metastasis staging in patients with malignant tumors: a meta-analysis of 13 prospective studies. *Ann Palliat Med* 2020; 9:247–255
37. Messiou C, Porta N, Sharma B, et al. Prospective evaluation of whole-body MRI versus FDG PET/CT for lesion detection in participants with myeloma. *Radiol Imaging Cancer* 2021; 3:e210048

38. Chen J, Li C, Tian Y, et al. Comparison of whole-body DWI and ¹⁸F-FDG PET/CT for detecting intramedullary and extramedullary lesions in multiple myeloma. *AJR* 2019; 213:514–523
39. Nishiyama Y, Kinuya S, Kato T, et al. Nuclear medicine practice in Japan: a report of the eighth nationwide survey in 2017. *Ann Nucl Med* 2019; 33:725–732

Editorial Comment: Visible and Occult Bone Lesions—Are They Really Different?

Radiologists are experienced and comfortable in performing skeletal biopsy, which is almost exclusively performed using CT guidance. However, biopsy of lesions that have been identified by MRI or by nuclear medicine studies, such as PET/CT, but that are occult on CT is a regular occurrence, completed through careful matching of target anatomy on CT to that on images showing the lesion [1]. Although newer biopsy methods such as MRI or PET/CT guidance may improve accuracy in obtaining tissue for both visible and occult lesions [2, 3], the dilemma remains of inconclusive or negative biopsy results and the interpretation of such information. The authors of this study address the problem of the occult bone lesion by examining the initial and final diagnoses in 70 occult lesions from a series of 1033 CT-guided nonaxial skeletal biopsies. Although diagnostic yield was only 37.1% among occult lesions, image review showed that all biopsies accurately targeted lesions. The real usefulness of this work therefore lies in the final diagnostic results gained through long-term follow-up.

Overall, occult lesions were significantly more likely to be benign than were visible lesions. Metastasis was the dominant malignant diagnosis among both visible and occult lesions. Among occult lesions, leukemia/lymphoma was also common, representing approximately a third of malignant diagnoses. Red or reactive marrow accounted for approximately 60% of benign occult lesions, compared with 20% of benign visible lesions; for occult lesions, diagnosis of these marrow changes required additional follow-up after the initial core needle biopsy in all cases.

Given ongoing increases in PET/CT and whole-body MRI use, occult bone lesions will be increasingly detected. CT-guided biopsy of these nonvisible lesions can be accurate and diagnostic. Knowledge of the frequencies of pathologic diagnoses can aid prebiopsy planning and guide multidisciplinary discussions regarding possible outcomes.

W. Bonner Guilford, MD
Charlotte Radiology
Charlotte, NC
bguil@bellsouth.net

Version of record: Oct 12, 2022

The author declares that there are no disclosures relevant to the subject matter of this article.

doi.org/10.2214/AJR.22.28207

Provenance and review: Solicited; not externally peer reviewed.

References

- Hillen TJ, Talbert RJ, Friedman MV, et al. Biopsy of CT-occult bone lesions using anatomic landmarks for CT guidance. *AJR* 2017; 209:214–221
- Li J, Zhou H, Zhang X, Song F, Pang X, Wei Z. A two-way comparison of whole-body ¹⁸F-FDG PET-CT and whole-body contrast-enhanced MRI for distant metastasis staging in patients with malignant tumors: a meta-analysis of 13 prospective studies. *Ann Palliat Med* 2020; 9:247–255
- Messiou C, Porta N, Sharma B, et al. Prospective evaluation of whole-body MRI versus FDG PET/CT for lesion detection in participants with myeloma. *Radiol Imaging Cancer* 2021; 3:e210048